Proceedings of the Pakistan Academy of Sciences: A Physical and Computational Sciences 61(2): 145-152 (2024)

ISSN (Print): 2518-4245; ISSN (Online): 2518-4253
http://doi.org/10.53560/PPASA(61-2)867

Pakistan Academy of Sciences

Research Article

Determination of Critical Slip Surface in Loose Rock Slope Stability Analysis

Zulkifl Ahmed[1], Sumra Yousuf[2*], Mahwish Zahra[3], Anum Aleha[3], Abid Latif[4], Tahir Sultan[4], Tanveer Ahmad Khan[2], and Muhammad Yousaf Raza Taseer[5]

[1]School of Resource and Civil Engineering, Northeastern University, Shenyang, China
[2]Department of Building and Architectural Engineering, Faculty of Engineering and Technology, Bahauddin Zakariya University, 60000 Multan, Pakistan
[3]Department of Architecture Design, National Fertilizer Corporation Institute of Engineering and Technology (NFC-IET), 60000 Multan, Pakistan
[4]Department of Civil Engineering, Faculty of Engineering and Technology, Bahauddin Zakariya University, 60000 Multan, Pakistan
[5]Department of Structure and Materials, Faculty of Civil Engineering, Universiti Teknologi Malaysia 81310, UTM, Johar, Malaysia

Abstract: Determination of representative Critical Slip Surface (CSS) for loose rock slope is one of the most important topics for slope reinforcement design. In this paper, a SLOPE/W software is used to analyze the failure characteristics of CSS considering the spatial variability effect of strength parameters. Initially, the Morgenstern-Price limiting equilibrium method was selected within the framework of SLOPE/W software to examine the failure mechanism of CSS and the corresponding Factor of Safety (FS) for a loose rock slope comprised of two different materials. Also, the variability effect of shear strength parameters (cohesion, friction angle) on minimum FS, the maximum depth (D), sliding arc length (L), distribution range of slip surfaces and slip surface entry point distance (D_e) were investigated through software. The results showed that all slip surfaces are mostly parallel and the local failure can happen at the top of the slope. Statistically, local failure has entry and exit points situated at the crest and near the toe of the slope, respectively. Shear strength parameters have a remarkable effect on FS, D, L and D_e of critical slip surface. The distribution range of CSS decreased with an increasing the amount of cohesion and friction angle. These findings can help to locate the actual position of CSS and slip surface entry point distance in case of loose rock slope.

Keywords: Morgenstern-Price Method, Failure Mechanism, Critical Slip Surface, FS, Entry Point Distance, Loose Rock.

1. INTRODUCTION

Engineers mostly simulate rock slope stability to precisely classify the most distinct critical slip surface. Engineers also use several analytical methods to evaluate the stability factor of natural or artificial slopes [1]. Limit equilibrium techniques are leading among these methods, in which the empirically based established site-stability charts may be applicable for slope stability calculation in certain conditions. In general, nevertheless, laboratory tests, field assessments and more precise numerical solutions are normally suggested. The outcomes of the above studies are usually reported as the probability of failure and Factor of Safety (FS) for the geotechnical structures [2, 3]. The shape of the sliding surface has been also widely used previously to determine the stability of various types of rock slopes. Such as circular arc shape was used to evaluate the stability of slopes [4]. The spiral slip surface was estimated for rock slope stability analysis [5], and the circular slip surface was determined for heterogeneous rock slope stability factor computation [6]. Other scholars

Received: March 2024; Revised: May 2024; Accepted: June 2024
* Corresponding Author: Sumra Yousuf <sumra.yousafrm@gmail.com>

have studied the stability of natural and or open pit slopes by ellipsoidal, revolution, cylindrical and critical circular slip surfaces [7-9].

In static analysis, the Critical Slip Surface (CSS) is the surface that produces the minimum FS during slope stability and the smallest value of FS can calculated by studying circular arc with cohesion (c) and friction (ϕ) parameters [10]. When a circular slip surface is studied, repeated trials can be done numerically. The greater difficulties involved in automating the search for non-circular surfaces. Most available computer programs that can be used to analyze and locate the most critical slip surface with repeated trials are more reliable for CSS determination. In most cases, only a circular slip surface was analyzed for general slope types when a computer program was used to perform the search automatically. In some cases, the most critical slip surface may not be approximated accurately by a circular arc [11]. In the cut slope case, the appropriate assumption is that the slip surface is repeated circular will result in an unknown. The method of judgment of the critical slip surface is directly connected to the method of determining the minimum Factor of Safety (FS). Some scholars have used limit equilibrium techniques to evaluate FS and critical slip surfaces statically [12-16], or numerically [17, 18]. To determine the minimum FS for a sliding surface, a general limiting equilibrium technique may allow a precise and accurate evaluation method during large-scale stability investigations. Therefore, commonly used approaches are limiting equilibrium techniques and cannot be used to locate CSS with general constrain under composite conditions. On the other hand, optimization techniques are considered an effective tool to estimate FS for single-slip surface [19]. On the other hand, dynamic programming is used to allocate the non-circular slip surface [18]. Monte-Carlo techniques can evaluate the FS of the critical slip surface of a slope [20]. Other researchers proposed some conventional solutions for rock slope stability analyses [21, 22].

In the current research, a simple geometrical method and GeoStudio software code are used to calculate the CSS and corresponding minimum FS. The failure mechanics for CSS are analyzed by varying the values of cohesion and friction. In this research, the CSS allocation provides concrete guidelines for choosing a typical sliding surface in risk assessments and system reliability analyses of heterogeneous rock slopes beside the road.

2. METHODOLOGY

In geotechnical engineering investigating the stability of slopes is also one of the oldest kinds of numerical study. In the mid of 20th century, [12-16] presented the knowledge of dividing the probable sliding mass into several number of slices. In the 1960 the dawn of computer technology made it conceivable to voluntarily switch the iterative measures essential in the scheme which controlled statistically more laborious equations for example those established previously [12-16]. In this research, SLOPE/W was selected which is a product of GeoStudio. One of the more commanding topographies of this joined method is that it provides access to sorts of investigations of a much more complex and broader field of difficulties, together with the use of stresses and calculated pore-water pressures in a stability study. It is possible in limit equilibrium (LE) computer programs such as SLOPE/W to deal with extremely irregular pore-water pressure conditions, complex stratigraphy, a variety of nonlinear and linear shear strength models, material heterogeneity, concentrated loads, structural reinforcement and practically any type of sliding surface shape.

2.1. General Limit Equilibrium Formulation

Figure 1 shows a representative sliding surface (AB), with arc length L, slices discretization scheme and the possible forces on a slice of a slope. Normal forces (E) and shear forces (X) are acting on the slice base and the slice sides respectively (Figure 1). Limit equilibrium (LE) calculation consists of two FS equations which permit the boundary of inter-slice normal-shear force conditions. One equation gives the FS regarding horizontal force equilibrium (F_f) while the other equation gives the

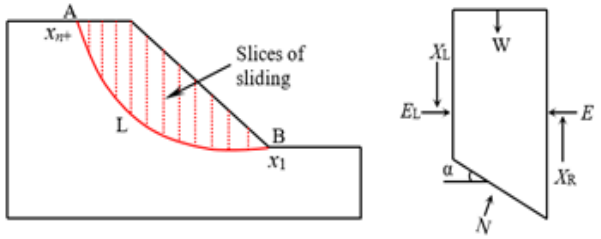

Fig. 1. Slice discretization and slice forces in a sliding mass.

FS about moment equilibrium (F_m). Morgenstern and Price [13] proposed an equation to handle inter-slice shear forces as:

$$X = E\lambda f(x) \quad (1)$$

Where, X = shear force, E = normal force, λ = dimensionless function and $f(x)$ = a function. In the current analysis a distinctive half-sine function was chosen and the *FS* equation relating to moment equilibrium is:

$$Fm = \frac{\sum(\acute{c}\beta R + (N - u\beta)\, R\tan\acute{\emptyset})}{\sum wx - \sum Nf \pm \sum Dd} \quad (2)$$

The FS equation regarding horizontal force equilibrium is:

$$Ff = \frac{\sum(\acute{c}\beta\cos\alpha + (N - u\beta)\tan\acute{\emptyset}\cos\alpha)}{\sum N\sin\alpha - \sum D\cos\omega} \quad (3)$$

And base normal is defined as:

$$N = \frac{W + (XR - XL) - \frac{(\acute{c}\beta\sin\alpha + u\beta\sin\alpha\tan\acute{\emptyset})}{F}}{\cos\alpha + \frac{\sin\alpha\tan\acute{\emptyset}}{F}} \quad (4)$$

In above equations ϕ' = effective internal angle of friction, c' = effective cohesion, N = base normal force, u = water pressure, W = slice weight, α = slice base inclination, D = point load and β, R, x, f, d, ω are geometric parameters.

Equation (4) is acquired with the summation of vertical forces. $F = Fm$ when base normal force N is substituted in Equation (2) and $F = F_f$ when N is substituted in Equation (3). The slice base normal force (N) is reliant on the inter-slice shear forces X_R and X_L on both sides of a slice. Limit equilibrium formulation calculates F_f and F_m as a choice of dimensionless function (λ) values. A plot is shown in Figure 2, computed with these values, which illustrates how F_f and F_m vary with lambda (λ). In the end, for the whole slope, there is only one *FS*. F_f and F_m were similar when both force and moment equilibrium were satisfied and also *FS* was the same in each slice.

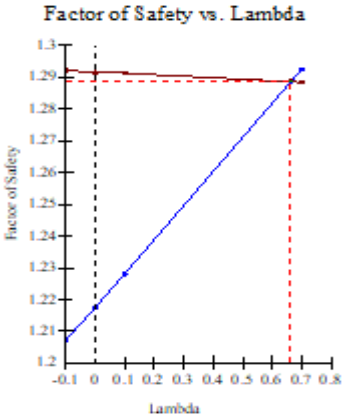

Fig. 2. Relationship between FS and λ.

3. NUMERICAL SIMULATION

3.1. Illustrative Example

A loose rock slope is located beside National Highway N70 in Pakistan considered as a case study. The slope material is composed of boulders as shown in Figure 3. It consists of 20-1000 mm diameter rounded rock pieces. This formation is valley floor sediment and is supposed to consist of two sandy layers. The total station was used to measure the boundaries and coordinates of the slope. Water pressure was measured with a piezometer. The coordinates of the water line are presented in Table 1.

3.2. Model Parameters

The width and height of the slope are 70 m and 35 m respectively as shown in Figure 4(a). A slope angle of 45° was recorded. The slope is composed of two different layers. The shear strength properties of slope material were estimated via direct shear test apparatus. The shear strength parameters were

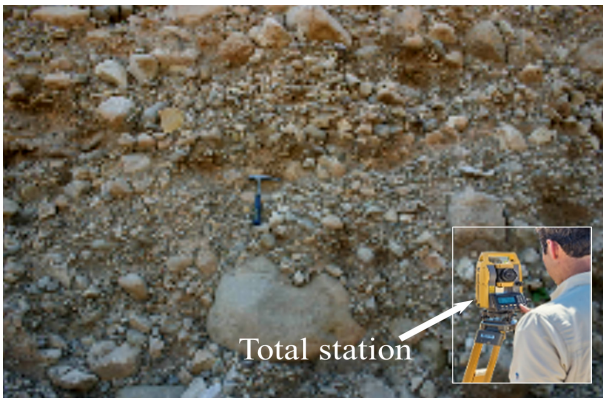

Fig. 3. Topography of loose rock slope and total station.

Table 1. Coordinates of piezo-metric line.

Coordinates	X(m)	Y(m)
1	0	22
2	30	17
3	52	13
4	70	13

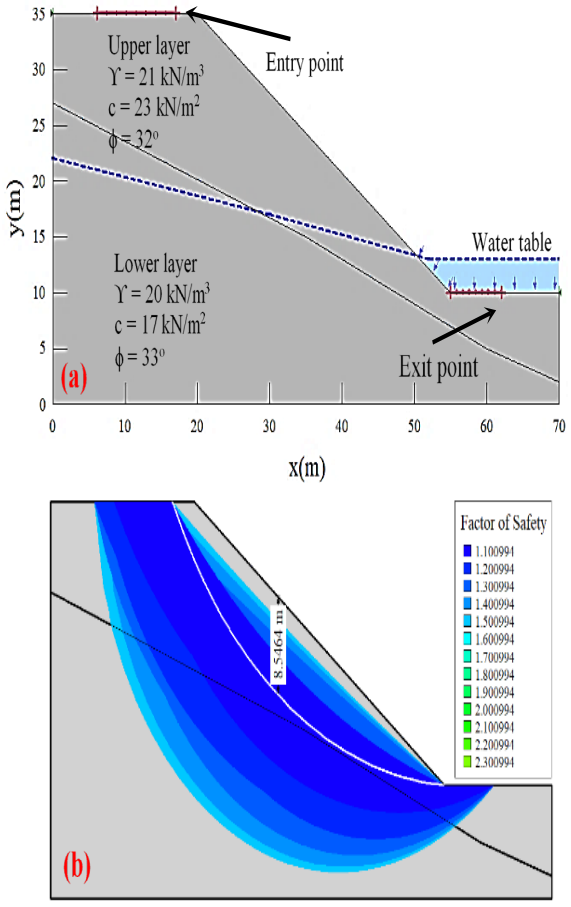

Fig. 4. (a) Slope model and (b) CSS in SLOPE/W analysis.

assigned to the corresponding region. The half-sin function and Mohr-Coulomb failure criterion are selected in a computer program (SLOPE/W) for further analysis. The trial slip surface entry and exit point were located according to Figure 4(a). The stability factor and the location of the CSS were then simulated by SLOPE/W software. Another effective way of graphically viewing a summary of the CSS is a safety map. The valid trial critical failure surface is shown with the factor of safety. This type of presentation clearly shows the location and distribution of the trial failure surface. Figure 4b shows that the critical failure surface initiates from the crest and cuts the slope near the toe.

3.3. Failure Characteristics of CSS

In this sub-section, the failure mechanism and the location of the critical slip surface are analyzed at various values of cohesion and friction angle. Failure mechanism of a critical failure surface can be acquired from a deterministic analysis and generating the different values of cohesion, and internal friction angle within the network of SLOPE/W software. Slope material is very loose and composed of two layers (upper layer and lower layer) of different materials. Three different cases are considered based on strength properties, namely, upper layer c = 16 (kN/m^2), ϕ = 21^o and γ = 17 (kN/m^3); c = 21 (kN/m^2), ϕ = 25^o and γ = 18 (kN/m^3) and c = 25 (kN/m^2), ϕ = 30^o and γ = 19 (kN/m^3) and lower layer c = 10 (kN/m^2), ϕ = 25^o and γ = 20 (kN/m^3); c = 15 (kN/m^2), ϕ = 30^o and γ = 21 (kN/m^3) and c = 20 (kN/m^2), ϕ = 35^o and γ = 21 (kN/m^3). Failure surface location and its failure mechanism for the three sets of input parameters (c, ϕ, γ) are plotted in Figure 5. The typical understandings have various aspects of CSS location by varying strength parameters. All CSSs are located between the crest and the toe of the slope and the failure of the slope is a local failure at an average value of strength parameters. CSS is plotted with the entry and exit method. The representative insights have different appearances of CSS failure and location and are categorized into three parts follows;

a. In the first case, the CSS was shallow and cut the toe of the slope as shown in Figure 5(a). The weak zone is comparatively small and is situated around the surface of the slope. The location of the CSS, in this case, is well dependable on the position of the weak zone and the overall failure style is a local failure. Because the factor of safety (FS) for the CSS passing through the weak zone is lesser than that for other slip surfaces representing an overall slope failure. When the failure of a slope surface happens in such a manner that the sliding surface cuts the slope surface or passes from the slope toe, it is called slope failure as shown in Figure 5(a, b). In this case, the slip surface entry and exit points are located near the top and on the toe of the slope respectively.
b. When the strength parameters were kept relatively large the CSS was deep. In the second case, the weak zones are relatively large and situated at the uppermost portion of the slope. The associated failure mechanism for a typical CSS is a narrow failure as shown in Figure 5(b). The judgment is that the FS is smaller for large sliding surfaces and running through the weak zone representing an overall failure.
c. When the large value of strength parameters is selected the CSS is located at a small distance from the toe of the slope and the failure mode is an overall failure. Because the FS for a CSS

is bigger as compared two other all valid slip surfaces in the weak areas of slope. In this case, the failure of the slope is a deep-seated failure and the location of CSS is not consistent with the location of the weak zone. The reason is that the load of a slope is a component of the gravity of the slope, which is proportional to the volume of the slide mass. The shear resistance of the slope consists of two parts, cohesion part and friction angle part. As the size of a sliding mass decreases, the decreasing rate of the associated CSS is smaller than that of the sliding volume. In other words, if the shear strength parameter remains constant and the size of the sliding mass decreases, the load of a slope decreases faster than the resistance of the slope. For a comparatively large repeated CSS as shown in Figure 5(c), the cohesion in the weak zone is small enough to generate FS smaller than the FS for an overall CSS.

It can be seen from the above analysis, that the failure mode for a heterogeneous slope with a relatively small value of strength parameters is an overall failure in most cases. Although local failures may happen in certain cases, the associated CSS always have entry points (the uppermost points of slip surfaces) located at the top of the slope and exit points (the lowermost points of slip surfaces) located near the toe of the slope.

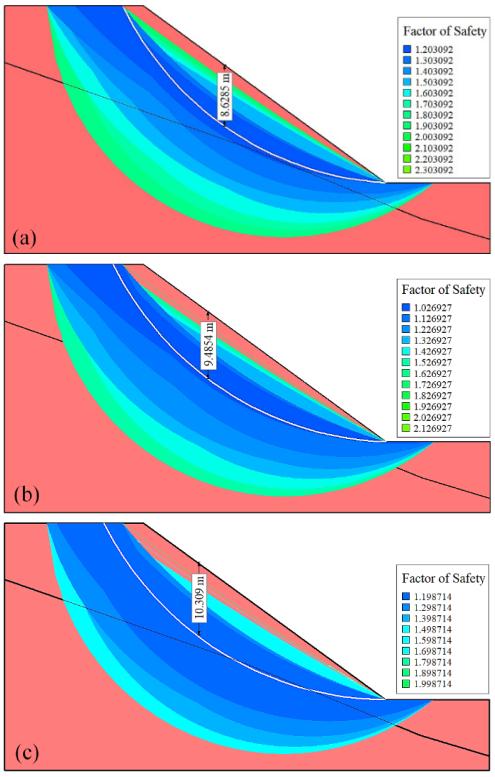

Fig. 5. Failure characteristics of critical slip surfaces, (a) small value of strength parameters, (b) comparatively large value of strength parameters, and (c) large value of strength parameters.

4. DISCUSSION

In this section, the distribution range of critical slip surfaces and corresponding FS are discussed by varying the values of c, and ϕ. The critical slip surface with an exit or an entry point on the face of the slope were assign as horizontal coordinates of the CSS uppermost part and lowermost part [17]. The distribution of CSS shows similar phenomena, and the results verified by Zhang *et al*. [23] study.

The influence of cohesion (c) and angle of internal friction (ϕ) on FS, depth (D), arc length (L) and its distribution are discussed in this subsection. First, the influence of cohesion is analyzed for the same slope model configuration. For this purpose, the unit weight (γ) and angle of internal friction (ϕ) are fixed to 20 kN/m^3 and 30^o, respectively. The value of cohesion (c) ranging from 10 kN/m^2 to 25 kN/m^2 is assigned in SLOPE/W. Four different slope models are tested by varying the values of cohesion as 10, 15, 20 and 25 (kN/m^2), respectively. The summary of computed safety factors and the depth (D) of CSS are graphically portrayed in Figure 6, which shows that all valid CSSs fall inside the range of trial slips.

The results exhibit that the FS value increases as increasing the value of the internal friction angle. Cohesion and friction have a significant influence on the FS of cut slope especially for greater values. The variability effect of c on FS, maximum depth (D) of CSS and distribution range of all valid CSSs were analyzed with different combinations of c, for both layers, which are plotted in Figure 6. For this purpose, three different cases based on c parameters are generated in SLOPE/W. The distribution range of SSs is consistent with the safety map.

As clearly shown in Figure 6(a–c), when the cohesion increased, there were big differences among the distributions of valid CSSs. In addition, the FS and maximum D increases linearly from 8. 55 m to 12.05 m. The reason is that the cohesion is a strength parameter increasing this value increase

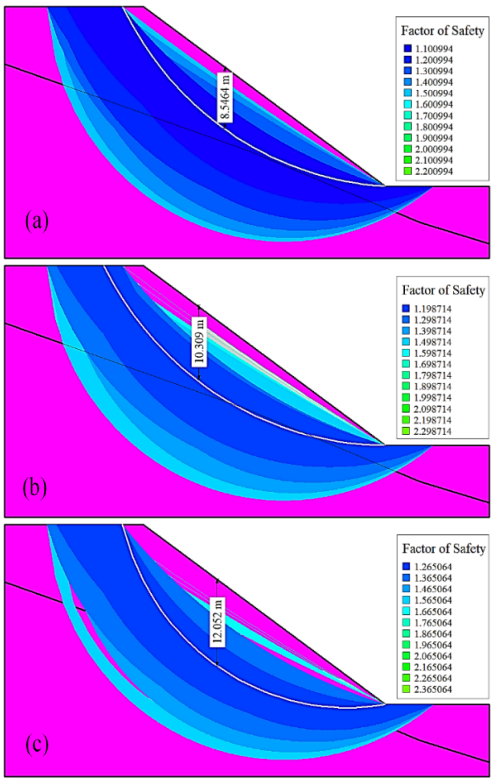

Fig. 6. Display of multiple trial slip surfaces, (a) small value of strength parameters, (b) comparatively large value of strength parameters, and (c) large value of strength parameters.

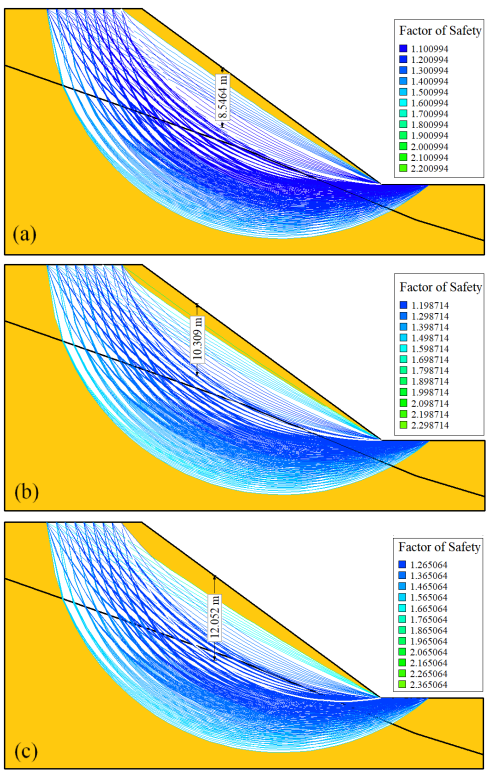

Fig. 7. Display of CSSs. (a) Small value of strength parameters, (b) comparatively large value of strength parameters and (c) large value of strength parameters.

in FS and depth of slip surface. In other words, very large or local CSSs are more likely to occur as the cohesion is large. Because cohesion is a strength parameter.

This paragraph examines the changeability influence of the angle of internal friction (ϕ) on the FS, maximum D and distribution range of CSSs. The same procedure for cohesion is adopted to investigate the effect of friction. By varying the value of friction angle, for both layers, three cases are investigated via SLOPE/W software. The variation of friction angle was set to be 20°, 25°, 30° and 25°, 30° and 35° for the upper and lower layers. The reason is that the value of ϕ varies from 20° and 35° for this particular case. Unit weight and cohesion are kept constant and are set to be 20 kN/m^3 and 15 kN/m^2, respectively. The effect of angle of internal friction on the distribution of CSS, D and FS is plotted in Figure 7. As the value of ϕ increased, the FS and depth and the distribution range of CSS also changed significantly. Local failures happened in the first two cases as ϕ = 20° and 25°, and 25° and 30° for both layers respectively (Figure 7 (a, b)). When the value of ϕ was 30° and 35° chosen, no local failure occurs as shown in Figure 7(c). The reason is that ϕ is a strength parameter increasing this increase in resistance force, which produced greater FS [1]. In other words, when the value of ϕ was large, All CSSs were extremely likely to enter the slope from the crest (entry point) and cut the slope near the toe. By contrast, when the value of ϕ was comparatively small, local failures have entry and exit points located on the crest and around the toe of the slope.

Slip surface entry point distance is an important parameter to define the reinforcement area of the slope. This is the distance from the crest to the failure point of slope as shown in Figure 8. The results of GeoStudio 2D software were used to determine slip surface entry point distance (D_e) and the length of failure arc (L) in the case of loose rock slope. The relationship between D_e and L and FS is plotted in Figure 9, where this can be established that L has an important influence on FS and D_e. It can be seen that entry point distance (D_e) and FS increased significantly as the L increased.

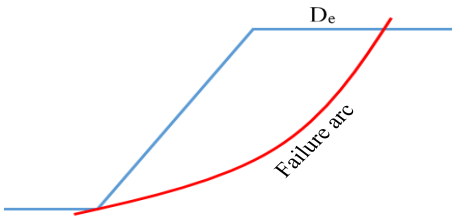

Fig. 8. Schematic diagram of the entry point distance (D_e) and length of failure surface.

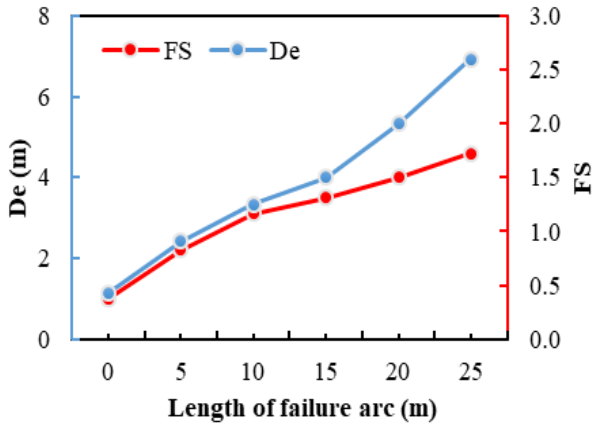

Fig. 9. Effect of entry point distance on the length of failure arc with corresponding FS.

Figure 9 is used to find the relation between entry point distance (D_e) and L, FS, slope height (h), γ, c and ϕ. The entry point distance (D_e) and L can be estimated using the following relations.

$$D_e = 0.89 \ln\left(\frac{c}{\gamma h \tan(\phi)}\right) + 3.2 \quad (5)$$

$$L = 0.81 \ln\left(\frac{c}{\gamma h \tan(\phi)}\right) + 6.19 \quad (6)$$

Where D_e is entry point distance of a CSS, c is cohesion in kN/m^2), γ is density of material, h is slope height (m), ϕ is internal friction angle of slope material and L is the length of slip surface.

5. CONCLUSIONS

In this study, the location of critical slip surfaces (CSS) in loose rock slope stability analysis was determined. The failure characteristics of CSS and the corresponding FS were also analyzed with the help of SLOPE/W software. The effect of cohesion (c), and internal friction (ϕ) on the failure mechanism of CSS and its depth (D) is also simulated. The following conclusions are drawn;

A loose rock slope can only show an overall failure by ignoring the shear strength properties. When the values of c and ϕ were small the circular failure did not occur and the CSS was a local one in case of loose rock slope. The location of CSS is consistent with the weak zone. Cohesion (c) and internal friction angle (ϕ) significantly affect the depth and length of CSS. Decreeing the value of c and ϕ results in a decrease in the length of the sliding arc (L). The shear strength parameters (c, ϕ) have a significant effect on the location of the critical slip surface and corresponding FS. Failure surface entry point distance (D_e) and the length of the sliding arc (L) have a logarithmic relationship with shear strength parameters. In future the effect of water pressure and earthquake loads must be considered for better understanding.

6. ACKNOWLEDGEMENTS

This work was conducted with the support of Bahauddin Zakariya University, Multan, Pakistan.

7. CONFLICT OF INTEREST

The authors declare no conflict of interest.

8. REFERENCES

1. M. Kinde, E. Getahun, and M. Jothimani. Geotechnical and slope stability analysis in the landslide-prone area: A case study in Sawla–Laska road sector, Southern Ethiopia. *Scientific African* 23: e02071 (2024).
2. X. Tang, C. Chen, D. Shan, P. Zhang, and J. Xue. Slope reliability assessment using an innovative critical failure path approach. *Frontiers in Earth Science* 12: 1428309 (2024).
3. A.S. Al-Jawadi. Predicting Slip Surfaces for Slope Stability Assessment Along Highway 80 in Mosul, Northern Iraq. *Geotechnical and Geological Engineering* 42(5): 2997–3008 (2024).
4. I. Khan, A. Afayou, N. Abbas, A. Khan, N. Alam, and S. Shah. Enhanced Geo-technical Methods for Evaluating Slope Stability in Unconsolidated Strata: A Comprehensive Analysis. *Journal of Mining and Environment* 15: 991-1010 (2024).
5. Z. Li, R. Wu, T. Hu, S. Xiao, L. Zhang, and D. Zhang. Stability analysis of an unstable slope in chongqing based on multiple analysis methods.

Processes 11: 2178 (2023).
6. M. Kassa, and M. Meten. Slope stability analysis using kinematic, limit equilibrium, and finite element models at Dessie town, northern Ethiopia. *Arabian Journal of Geosciences* 16: 675 (2023).
7. L. Li, Y. Wang, L. Zhang, C. Choi, and C. Ng. Evaluation of critical slip surface in limit equilibrium analysis of slope stability by smoothed particle hydrodynamics. *International Journal of Geomechanics* 19: 04019032 (2019).
8. J. Zhang, and H. Huang. Risk assessment of slope failure considering multiple slip surfaces. *JC Geotechnics* 74: 188-95 (2016).
9. P.R. Kumar, K. Muthukkumaran, and C. Sharma. Technological Advancements and Sustainable Practices in Rock Slope Stability–Critical Review. *Chemistry of the Earth* 136: 103699 (2024).
10. M. Hajiazizi, and H. Tavana. Determining three-dimensional non-spherical critical slip surface in earth slopes using an optimization method. *Engineering Geology* 153: 114-124 (2013).
11. R. Baker. Determination of the critical slip surface in slope stability computations. *International Journal for Numerical and Analytical Methods in Geomechanics* 4: 333-59 (1980).
12. A.W. Bishop. The use of the slip circle in the stability analysis of slopes. *Geotechnique* 10: 129-150 (1955).
13. N. Morgenstern, and V.E. Price. The analysis of the stability of general slip surfaces. *Geotechnique* 15: 79-93 (1965).
14. E. Spencer. A method of analysis of the stability of embankments assuming parallel inter-slice forces. *Geotechnique* 17: 11-26 (1967).
15. A. Bishop, and N. Morgenstern. Stability coefficients for earth slopes. *Geotechnique* 10: 129-153 (1960).
16. O. Hungr, F. Salgado, and P. Byrne. Evaluation of a three-dimensional method of slope stability analysis. *Canadian Geotechnical Journal* 26: 679-86 (1989).
17. X. Qi, and D. Li. Effect of spatial variability of shear strength parameters on critical slip surfaces of slopes. *Engineering Geology* 239: 41-9 (2018).
18. P. Regmi, and K. Jung. Application of dynamic programming to locate the critical failure surface in a rainfall induced slope failure problem. *KSCE Journal of Civil Engineering* 20: 452-62 (2016).
19. H. Pham, and D. Fredlund. The application of dynamic programming to slope stability analysis. *Canadian Geotechnical Journal* 40: 830-47 (2003).
20. A. Malkawi, W. Hassan, and S. Sarma. Global search method for locating general slip surface using Monte Carlo techniques. *Journal of Geotechnical and Geoenvironmental Engineering* 127: 688-98 (2001).
21. H. Zheng, D. Liu, and C. Li. Slope stability analysis based on elasto-plastic finite element method. *International Journal for Numerical Methods in Engineering* 64: 1871-88 (2005).
22. Y. Cheng, T. Lansivaara, and W. Wei. Two-dimensional slope stability analysis by limit equilibrium and strength reduction methods. *Computers and Geotechnics* 34: 137-50 (2007).
23. W. Zhang, Q. Zhao, J. Chen, R. Huang, and X. Yuan. Determining the critical slip surface of a fractured rock slope considering preexisting fractures and statistical methodology. *Landslides* 14: 1253-63 (2017).